VIII International Conference on Particle-Based Methods
PARTICLES 2023
U. Perego, M. Cremonesi, A. Franci (Eds)

NON-FOURIER HEAT CONDUCTION WITH PHASE CHANGE USING HYPERBOLIC LATTICE BOLTZMANN METHOD BY MODIFYING THE EQUILIBRIUM DISTRIBUTION FUNCTION

Snehil Srivastava[1], **Panchatcharam Mariappan** [1*]

[1] Department of Mathematics and Statistics, Indian Institute of Technology, Tirupati, 517619, Andhra Pradesh, India. e-mail: MA19D002@iittp.ac.in

Abstract: The study presented a simulation of non-Fourier heat conduction with phase change using a hyperbolic lattice Boltzmann method (HLBM). To handle the latent-heat source term, the equilibrium distribution function was modified for the temperature, leading to a novel approach. Unlike the conventional lattice Boltzmann method (LBM), the HLBM process employed a hyperbolic collision operator. This innovative approach facilitated the retrieval of the enthalpy conservation equation without the need for iteration stages or solving groups of linear equations. Consequently, this method demonstrated enhanced efficiency and accuracy compared to previous approaches.

The research showcased the potential of employing HLBM in simulating intricate thermal processes, especially those involving phase change. The approach's applicability extends to various domains, including designing efficient heat exchangers and gaining insights into material behavior during phase transitions. The findings suggest that HLBM holds promise as a valuable tool for addressing complex thermal phenomena and advancing our understanding of such processes.

Keywords. Phase change, Hyperbolic Lattice Boltzmann method, Equilibrium distribution function

1 INTRODUCTION

A phase change is a significant issue in engineering applications, such as energy storage and alloy solidification. Although the differential equation can help determine the type of phase changes, its non-linear nature makes it challenging to solve analytically. Consequently, numerical approaches have been developed as viable solutions, since analytical solutions are generally restricted to simple geometry and boundary constraints. The progress in microscale processing technology has drawn significant interest in dealing with solid-liquid phase problems involving microscale alterations, like laser cutting [1] and selective laser melting (SLM) [2]. Scholars have put forward numerous numerical methods to tackle the intricacies of the phase transition process. These methods can be classified into two groups: those that employ a fixed grid to analyze the solid-liquid interface and those that utilize a warped mesh or modified coordinates. However, the distorted mesh approach has certain drawbacks, such as complex coding and long processing times, in

contrast to the fixed grid method. Voller et al. [1] have discussed several fixed grid approaches for solving phase change problems. However, the enthalpy approach and the equivalent heat capacity method [2] are the two most commonly used fixed grid methods.

One of the numerical methods used to solve phase change problems is the Lattice Boltzmann method (LBM). Many authors have coupled the enthalpy method with LBM to address these problems. Jiaung et al. [3] employed an iterative strategy to handle the source term and directly obtain the temperature to find a solution to the phase change problem. Gorla et al. [4] utilized a double distribution function approach coupled with the Enthalpy method to solve the phase change problem. Chaterjee et al. [5] presented a method for simulating phase change by coupling a passive scalar-based thermal Lattice Boltzmann model with a fixed grid porosity approach. Additionally, a new Lattice Boltzmann model for solid-liquid phase change has been proposed by [6], which modifies the equilibrium distribution function for the temperature to handle the latent heat source term

The LBM-BGK format proposed by Bhatnagar-Gross-Krook solely takes into account the Fourier effect and ignores all other effects. To overcome this, Cattaneo [7] and Vernotte [8] developed the CV model, which solves the hyperbolic heat equation while taking into consideration the non-Fourier effect.[9] suggested the hyperbolic lattice Boltzmann technique (HLBM) to get around this, and for that, the hyperbolic collision operator entered the picture. [10] brought out the concept of one-dimensional (1D) non-Fourier heat conduction with phase change using HLBM.

To avoid the challenges associated with the iterative technique used in [3], this paper proposes a method that combines the latent heat source term into the transient term. The approach involves modifying the equilibrium distribution function and developing an HLBM model based on the governing equation. With this method, the temperature can be directly calculated for 1D and 2D Fourier and non-Fourier heat conduction phenomena with phase change.

2 Governing Equations

The enthalpy method is widely acknowledged as one of the most efficient approaches for modeling solid-liquid phase change problems. The governing equations representing the enthalpy formulation of phase change are as follows:

$$\frac{\partial(\rho C_p T)}{\partial t} = \nabla.(K\nabla T) - L_a \frac{\partial(\rho f_l)}{\partial t} \tag{1}$$

In this context, the variables ρ, K, and T stand for density, thermal conductivity, and temperature, respectively. Additionally, C_p, L_a, and f_l represent specific heat capacity at constant pressure, latent heat of phase change, and the liquid phase fraction, respectively. The left-hand side of equation (1) accounts for the transient term, while the last term on the right-hand side is referred to as the latent heat term.

By combining the latent heat term and the transient term, we can derive the total enthalpy-based energy governing equation. This equation, which is a reformulation of Equation (1), is given by:

$$\frac{\partial H}{\partial t} = \nabla.\left(\frac{K}{\rho}\nabla T\right) \tag{2}$$

In this equation, H represents the total enthalpy and is defined as the sum of the product of the specific heat capacity at constant pressure (C_p) and temperature (T) with the liquid phase fraction (f_l) multiplied by the latent heat of phase change (L_a):

$$H = C_p T + f_l L_a$$

3 Hyperbolic Lattice Boltzmann method for heat conduction with phase change

3.1 CV Heat Conduction Problem

Combining the latent heat source term $\partial_t(\rho_0 L f_l)$ into the transient term $\partial_t(\rho_0 c_p T)$, The CV heat transfer total enthalpy-based energy governing equation as

$$\frac{\partial H}{\partial t} + \tau\frac{\partial^2 H}{\partial t^2} = \alpha\nabla.(C_p\nabla T) \tag{4}$$

Equation (4) can be rewritten as:

$$\frac{\partial H}{\partial t} = \frac{\alpha}{1+\tau\frac{\partial}{\partial t}}\nabla^2(C_p T) \tag{5}$$

The equation (4) LBM form is

$$g_i(x + c_i\Delta t, t + \Delta t) - g_i(x,t) = \Lambda[g_i(x,t) - g_i^0(x,t)] \tag{6}$$

In this case, g_i and g_i^0 represent the particle distribution function and equilibrium distribution function in the i^{th} direction, respectively. The time step is denoted as Δt, the lattice size is represented by Δx, and the collision operator we need is referred to as Λ.

$$g_i^0 = \begin{cases} H - C_p T + w_i C_p T & i = 0 \\ w_i C_p T & i \neq 0 \end{cases}$$

The weight functions corresponding to each distribution function are labeled as w_i.

The Taylor series expansion of $g_i(x + c_i\Delta t, t + \Delta t)$ around (x,t) is given as:

$$\begin{aligned} g_i(x + c_i\Delta t, t + \Delta t) = {} & g_i(x,t) + \Delta t\partial_t g_i + \Delta t\partial_{x_\alpha} c_{i_\alpha} g_i \\ & + \frac{1}{2}(\Delta t)^2(\partial_t\partial_t g_i + 2\partial_t\partial_{x_\alpha} c_{i_\alpha} g_i + \partial_{x_\alpha}\partial_{x_\beta} g_i) + O(\Delta t^3) \end{aligned} \tag{7}$$

The variables x_α, x_β represent the components of the vector $\mathbf{x}$ in the x and y directions, respectively. In addition, the variables $c_{i\alpha}$ and $c_{i\beta}$ represent the velocities in the x and y directions respectively. Substituting equation (7) in equation (6) gives:

$$\begin{aligned} \Delta t\partial_t g_i + \Delta t\partial_{x_\alpha} c_{i_\alpha} g_i + \frac{1}{2}(\Delta t)^2(\partial_t\partial_t g_i + 2\partial_t\partial_{x_\alpha} c_{i_\alpha} g_i + \partial_{x_\alpha}\partial_{x_\beta} g_i) \\ = \Lambda[g_i(x,t) - g_i^0(x,t)] \end{aligned} \tag{8}$$

The distribution function has the following constraints:

$$\sum_i g_i^0 = H \tag{9}$$

$$\sum_i g_i^r = 0, (r \geq 1) \tag{10}$$

$$\sum_i \mathbf{c_i c_i} g_i^0 = C_p T C_s^2 \tag{11}$$

The variable r is used to denote higher-order derivatives, while the symbol C_s represents the speed of the lattice. By introducing the Knudsen number ϵ [11], provides the following equations Introducing the Knudsen number ϵ [11]

$$\partial_t = \epsilon^2 \partial_{t^{(2)}}, \partial_{\mathbf{x}} = \epsilon \partial_{\mathbf{x^{(1)}}} \tag{12}$$

The parameter $t^{(2)}$ represents the slow time scale related to the diffusive process, while $\mathbf{x^{(1)}}$ represents the corresponding relatively large spatial scale. The expansion of $g_i(x,t)$ is involved in this context.

$$g_i = g_i^{(0)} + \epsilon g_i^{(1)} + \epsilon^2 g_i^{(2)} + O(\epsilon^3) \tag{13}$$

Substituting (12) in (8) and truncating the terms with an order of magnitude larger than $O(\epsilon^3)$. To recover (4), summation over all states for (8) is given as:

$$\sum_i \epsilon^2 \Delta t \partial_t^{(2)} g_i + \sum_i \epsilon \Delta t \partial_{x_\alpha^{(1)}} c_{i_\alpha} g_i + \sum_i \frac{1}{2} \Delta t^2 \epsilon^2 c_{i_\alpha} c_{i_\beta} \partial_{x_\alpha^{(1)}} \partial_{x_\beta^{(1)}} g_i = \Lambda \Big(\sum_i (g_i(x,t) - g_i^{eq}(x,t)) \Big) \tag{14}$$

The first term on the LHS of (14) corresponds to the unsteady term as:

$$\sum_i \epsilon^2 \Delta t \partial_t^{(2)} g_i = \sum_i \Delta t \partial_t g_i = \Delta t \partial_t H \tag{15}$$

The second term on the LHS of (14) is given as:

$$\begin{aligned}
\sum_i \epsilon \Delta t \partial_{x_\alpha^{(1)}} c_{i_\alpha} g_i &= \sum_i \epsilon \Delta t \partial_{x_\alpha^{(1)}} c_{i_\alpha} \left[g_i^0 + \epsilon g_i^1 + O(\epsilon^2) \right] \\
&= \epsilon \Delta t \partial_{x_\alpha^{(1)}} \sum_i c_{i_\alpha} g_i^{(0)} + \epsilon^2 \Delta t \partial_{x_\alpha^{(1)}} \sum_i c_{i_\alpha} g_i^{(1)} + O(\epsilon^3) \\
&= \epsilon \Delta t \partial_{x_\alpha^{(1)}} \sum_i c_{i_\alpha} \left(\frac{1}{\Lambda} \epsilon \partial_{x_\beta^{(1)}} c_{i_\beta} g_i^0 \right) = \epsilon^2 \Delta t^2 \frac{1}{\Lambda} \partial_{x_\alpha^{(1)}} \partial_{x_\beta^{(1)}} c_{i_\alpha} c_{i_\beta} g_i^{(0)} \\
&= \frac{\Delta t^2}{\Lambda} c^2 \nabla^2 T (D1Q2) \\
&= \frac{\Delta t^2}{3\Lambda} c^2 \nabla^2 T (D2Q5)
\end{aligned}$$

The third term on LHS of (14) becomes:

$$\begin{aligned}
&\frac{1}{2}\Delta t^2\epsilon^2\sum_i c_{i_\alpha}c_{i_\beta}\partial_{x_\alpha^{(1)}}\partial_{x_\beta^{(1)}}g_i \\
&\qquad = \frac{1}{2}\Delta t^2\sum_i \epsilon^2 c_{i_\alpha}c_{i_\beta}\partial_{x_\alpha^{(1)}}\partial_{x_\beta^{(1)}}\left[g_i^0+\epsilon f_i^1+O(\epsilon^2)\right] \\
&\qquad = \frac{1}{2}\Delta t^2\epsilon^2\partial_{x_\alpha^{(1)}}\partial_{x_\beta^{(1)}}\sum_i c_{i_\alpha}c_{i_\beta}g_i^{(0)}+O(\epsilon^3) \\
&\qquad = \frac{\Delta t^2}{2}c^2\nabla^2 T(D1Q2) \\
&\qquad = \frac{\Delta t^2}{6}c^2\nabla^2 T(D2Q5)
\end{aligned}$$

The RHS of (14) is:

$$\Lambda\big(\sum_i g_i-\sum_i g_i^{eq}\big)=\Lambda(H-H)$$

Thus, (14) becomes:

$$\frac{\partial H}{\partial t}=-\left(\frac{1}{\Lambda}+\frac{1}{2}\right)\Delta t c^2\nabla^2 T \tag{16}$$

Comparing equation (5) and equation (16)

$$-\left(\frac{1}{\Lambda}+\frac{1}{2}\right)\Delta t c^2=\frac{\alpha}{1+\tau\frac{\partial}{\partial t}} \tag{17}$$

The Hyperbolic collision operator Λ is given by:

$$\Lambda=-\frac{2\left(1+\tau\frac{\partial}{\partial t}\right)}{2\alpha^*+\left(1+\tau\frac{\partial}{\partial t}\right)} \tag{18}$$

Substituting the value of Λ in equation (6)

$$\psi_i=\phi\psi_i^0-2(\phi+\varphi)\theta_i+2\phi\theta_i^0 \tag{19}$$

Here, $\psi_i(x,t)=g_i(x+\Delta x,t+\Delta t)-g_i(x,t)$, $\psi_i^0(x,t)=\psi_i(x,t-\Delta t)$, $\theta_i(x,t)=g_i(x,t)-g_i^{eq}(x,t)$, $\theta_i^0=\theta_i(x,t-\Delta t)$, $c=\frac{\Delta x}{\Delta t}$, $\alpha^*=\frac{\alpha_1}{\Delta t c^2}$, $\phi=\frac{\gamma}{2\alpha^*+1+\gamma}$, $\varphi=\frac{1}{2\alpha^*+1+\gamma}$, $\gamma=\frac{\tau}{\Delta t}$

The operator Λ is commonly referred to as the hyperbolic collision operator, and the lattice Boltzmann method utilizing this operator is recognized as the hyperbolic lattice Boltzmann method (HLBM).

3.2 Method

3.2.1 Lattice arrangement

In the collision phase of HLBM, the collision operator is used to calculate the rate of change of the distribution functions, which describe the probability of particles having certain velocities at a given point in space and time. The collision operator is derived from the governing equations of fluid dynamics and accounts for the interactions between particles.

During the streaming phase, the distribution functions propagate to neighboring nodes on a lattice based on a set of discrete velocities.

D1Q2 and D2Q5 are two different lattice models as shown in figure (1). In LBM, a fluid is represented by a set of discrete velocities on a lattice, and the dynamics of the fluid are simulated by tracking the evolution of the distribution functions associated with these velocities.

D1Q2 model is a 1D model with two discrete lattice velocities (c_0 and c_1), and two distribution functions (f_0 and f_1) associated with these velocities. It is a simple model used to simulate fluid flow in one dimension.

On the other hand, the D2Q5 model is a 2D model with five discrete lattice velocities (c_0, c_1, c_2, c_3, and c_4), and five distribution functions (f_0, f_1, f_2, f_3, and f_4) associated with these velocities. It is a more complex model used to simulate fluid flow in two dimensions.

In general, the choice of the lattice model depends on the specific problem being simulated and the accuracy and efficiency required.

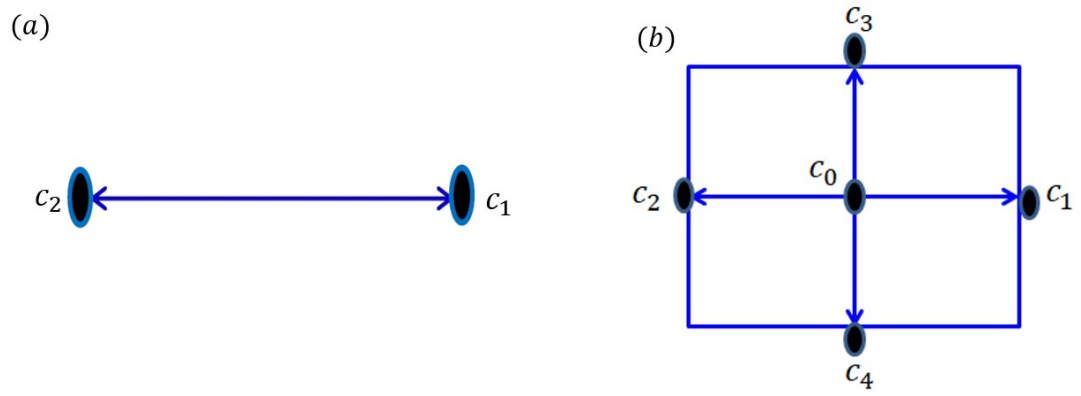

Figure 1: Details of lattice arrangement. Panels (a) and (b) showing the D1Q2 and D2Q5 configurations, respectively.

4 Results and Discussion

The provided excerpt explores the utilization of HLBM to investigate a heat conduction problem involving phase change, which deviates from the conventional Fourier heat

conduction. The study highlights the LBM's effectiveness in dealing with Fourier heat conduction and the HLBM's capability in handling more sophisticated cases incorporating relaxation time (τ). The developed model in this research simplifies coding complexity and facilitates the extraction of enthalpy and temperature from the equilibrium distribution function.

4.1 Solidification in 1D half space (One region problem)

The schematic diagram shows a 1D system undergoing a phase change from liquid to solid state. The system is initially at a temperature T_m and in a liquid state, and the temperature abruptly decreases to T_0 at $x = 0$ at time $t = 0$. The temperature is then held constant at T_0 for all times $t > 0$. The liquid-solid interface, denoted by the dashed line, moves in the positive x direction as solidification progresses.

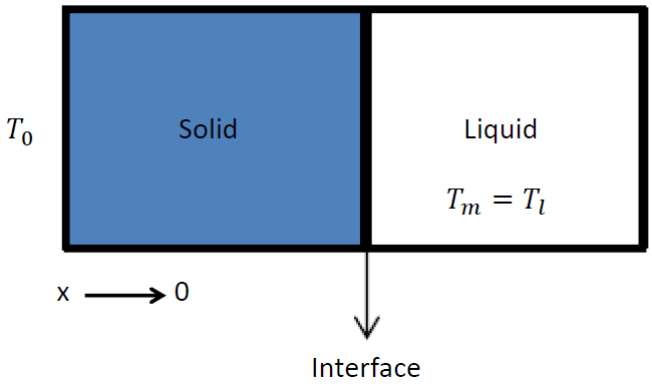

Figure 2: Schematic diagram of solid-liquid phase change problem

4.1.1 Fourier heat conduction with phase change

We set $\tau = 0$ to verify the accuracy of the phase change method used to demonstrate the solidification phenomenon. This simplifies the system to the Fourier heat conduction with phase change, whose analytical solution is available in [12]. Initially, the system's temperature is at the melting point $T_m = 0$ and subsequently cooled to $T_0 = -1$ while releasing latent heat $L_a = 0.01$, with a thermal diffusivity of $\alpha = 0.05$. The temperature distribution is presented in Figure (3), which agrees closely with the analytical solution. This agreement provides evidence for the accuracy of the simulation studying the solidification phenomenon.

4.1.2 non-Fourier heat conduction with phase change

In this study, we observe non-Fourier heat conduction with phase change, which differs from Fourier heat conduction due to the impact of relaxation time τ. The physical

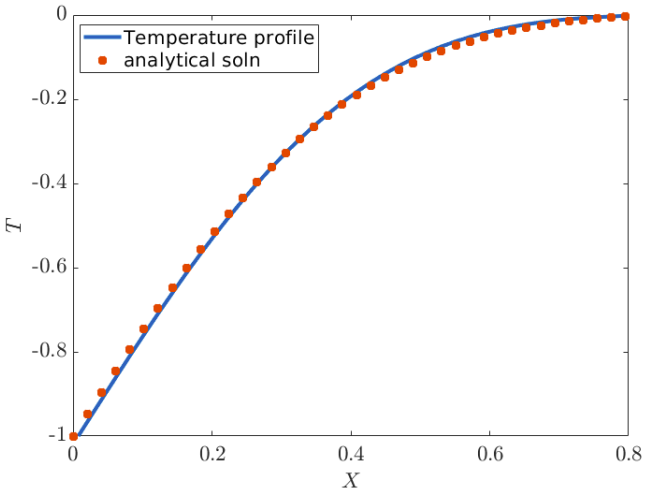

Figure 3: Comparison between Analytical and HLBM solution

parameters selected for the investigation are $T_m = 0$, $T_0 = -1$ and $\alpha_1 = 0.05$. The temperature distribution resulting from this setup is illustrated in Figure (4). Thermal diffusivity is a physical property that describes the ability of a material to conduct heat relative to its ability to store heat. Materials with high thermal diffusivity are able to rapidly conduct heat, while materials with low thermal diffusivity are slower to conduct heat. It is observed that as the α increases, the solidification process increases too and is shown in figure (8).

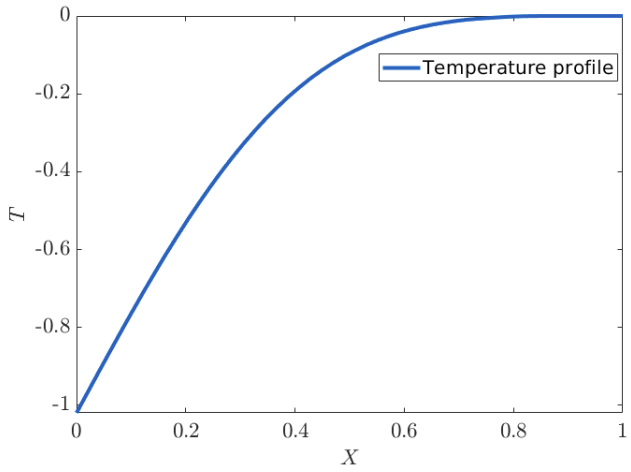

Figure 4: Temperature distribution using HLBM

4.2 Solidification in the square cavity (One region problem)

The solidification process involves the transformation of a substance from a liquid to a solid state. In this specific scenario, a square-shaped cavity is employed to aid in the

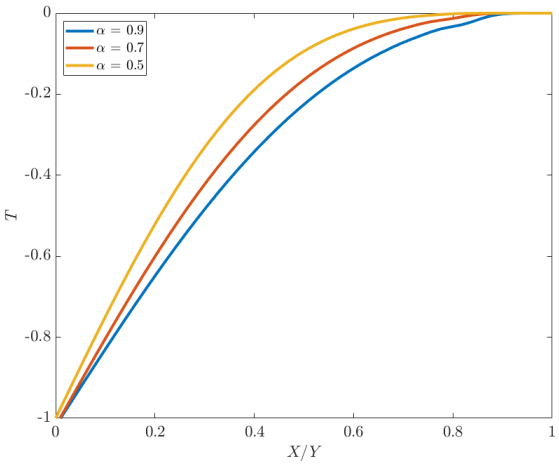

Figure 5: Temperature distribution using HLBM at various $\alpha_s^{'}$

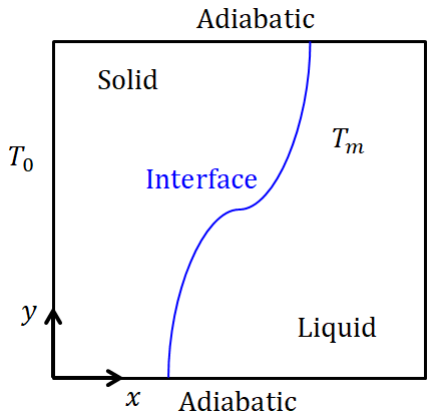

Figure 6: Schematic diagram of solid-liquid phase change problem.

solidification process. Initially, at time $t = 0$, the substance exists in a liquid state, and its phase change temperature T_m apply to the regions where $x > 0$ and $y > 0$. However, the temperature at $x = 0$ and $y = 0$ gradually decreases until it reaches T_0, after which it remains constant for all subsequent times $t > 0$. Consequently, the left side of the interface solidifies while the right side remains in a liquid state. This situation is known as a one-region problem because the temperature in one phase is already known, and the temperature in the other phase is the only parameter of interest. Refer to Figure (6) for the schematic diagram of the process.

4.2.1 Solidification in Half Region (HLBM)

This case involves observing the 2D non-Fourier heat conduction phenomenon, which takes into account the impact of relaxation time. The physical parameters used in this scenario are as follows: $\tau = 0.1$, $T_0 = -1$, $T_m = 0$, and $\alpha = 0.05$. It is assumed that the

material properties are constant. The temperature profile at time $t = 1$ is depicted in Figure (7). This non-Fourier heat conduction phenomenon is a more accurate representation of heat transfer in some materials, particularly in cases where there are high-temperature gradients or short-time scales involved. By considering the contribution of relaxation time, this model can more accurately predict the temperature distribution in such cases

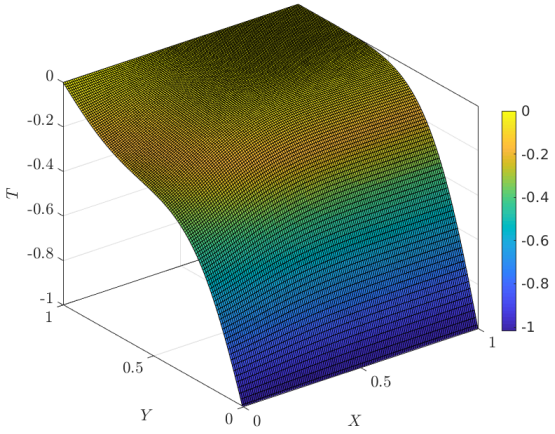

Figure 7: Temperature distribution of 2D CV heat conduction problem with phase change using HLBM

4.3 Effect of Thermal diffusivity

Thermal diffusivity (α) plays a crucial role in determining the rate of heat transfer through a medium. By varying the value of α and studying the resulting temperature profiles, we have observed that increasing the thermal diffusivity leads to a significant improvement in the solidification process. This can be attributed to the fact that higher thermal diffusivity allows for faster and more efficient heat transfer, resulting in faster cooling rates and finer microstructures. The temperature distribution at different values of α can be seen in Figures (8) and (9).

5 Conclusion

The solidification problem was tackled in this paper using the total enthalpy-based energy equation, and modifications were made to the equilibrium distribution function. This model was then integrated with HLBM to study the 1D and 2D Fourier and non-Fourier heat conduction phenomena. Additionally, the effect of changing α_s' on temperature was also examined. By employing this approach, we were able to gain a better understanding

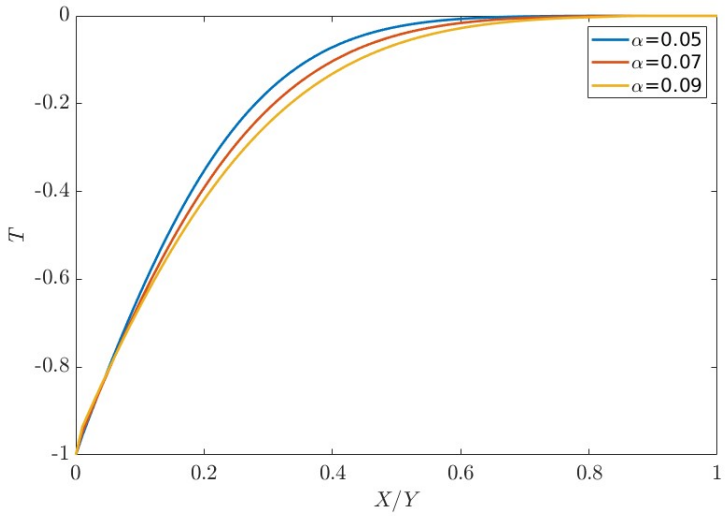

Figure 8: Temperature distribution of 2D CV heat conduction problem with phase change using HLBM at various $\alpha_s^{'}$

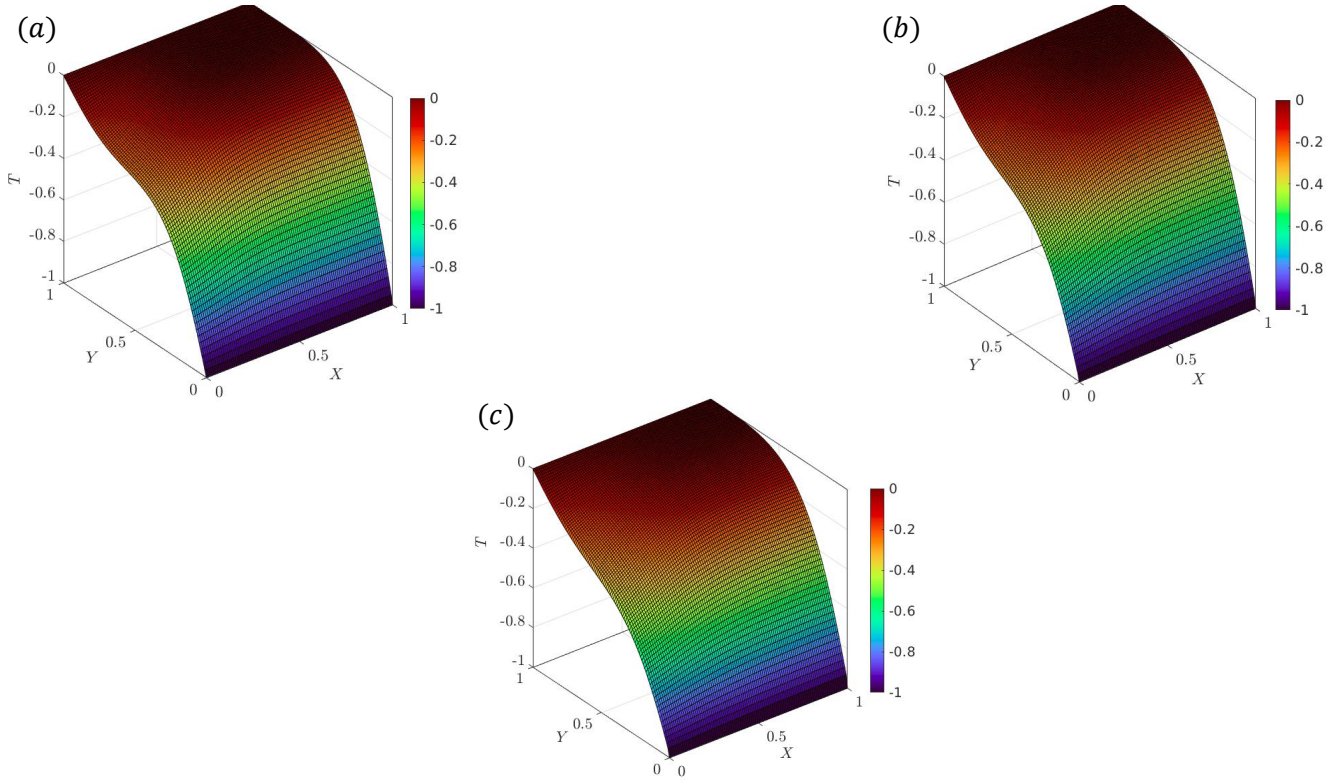

Figure 9: Details of Temperature distribution. Panel (a) $\alpha = 0.05$, panel (b) $\alpha = 0.07$, and, panel (c) $\alpha = 0.09$

of the solidification process and the various factors that influence it. The use of the total enthalpy-based energy equation and modified equilibrium distribution function provides a more accurate representation of the heat transfer process, and the combination with HLBM allows for a more efficient and accurate simulation of the solidification problem.

REFERENCES

[1] Vaughan R Voller, CR Swaminathan, and Brian G Thomas. Fixed grid techniques for phase change problems: a review. *International journal for numerical methods in engineering*, 30(4):875–898, 1990.

[2] Comini Bonacina, G Comini, A Fasano, and M 1973 Primicerio. Numerical solution of phase-change problems. *International Journal of Heat and Mass Transfer*, 16(10):1825–1832, 1973.

[3] Chun-Pao Kuo Wen-Shu Jiaung, Jeng-Rong Ho. Lattice boltzmann method for the heat conduction problem with phase change. *Numerical Heat Transfer, Part B: Fundamentals*, 39(2):167–187, 2001.

[4] Ahmed Ibrahem. Lattice boltzmann technique for heat transport phenomena coupled with melting process. *Heat and Mass Transfer*, 52, 01 2017.

[5] Dipankar Chatterjee. *Lattice Boltzmann Modeling for Melting/Solidification Processes*. 10 2011.

[6] Rongzong Huang, Huiying Wu, and Ping Cheng. A new lattice boltzmann model for solid-liquid phase change. *International Journal of Heat and Mass Transfer*, 59:295–301, 04 2013.

[7] Carlo Cattaneo. Sulla conduzione del calore. *Atti Sem. Mat. Fis. Univ. Modena*, 3:83–101, 1948.

[8] Pierre Vernotte. Sur quelques complications possibles dans les phenomenes de conduction de la chaleur. *Compte Rendus*, 252:2190–2191, 1961.

[9] Yi Liu, Ling Li, and Qin Lou. A hyperbolic lattice boltzmann method for simulating non-fourier heat conduction. *International Journal of Heat and Mass Transfer*, 131:772–780, 2019.

[10] Yi Liu and Ling Li. Lattice boltzmann simulation of non-fourier heat conduction with phase change. *Numerical Heat Transfer, Part A: Applications*, 76(1):19–31, 2019.

[11] A. A. Mohamad. *The Boltzmann Equation*. Springer London, London, 2019.

[12] M. N. Ozisik. *Heat Conduction (2nd ed.)*. Wiley, New York, 1993.